MolecularMedicine

MicroRNA-15a/16 Regulates Apoptosis of Lung Epithelial Cells After Oxidative Stress

Yong Cao,[1,2] Duo Zhang,[1] Hyung-Geun Moon,[1] Heedoo Lee,[1] Jeffrey A Haspel,[3] Kebin Hu,[4] Lixin Xie,[5] and Yang Jin[1]

[1]Division of Pulmonary and Critical Care Medicine, Pulmonary Center, Boston University Medical Campus, Boston, Massachusetts, United States of America; [2]Department of Respiratory Medicine, Tongji Hospital, Tongji Medical College, Huazhong University of Science and Technology, Wuhan, People's Republic of China; [3]Department of Medicine, Washington University School of Medicine, St. Louis, Missouri, United States of America; [4]Department of Medicine, Penn State University College of Medicine, Hershey, Pennsylvania, United States of America; and [5]Department of Respiratory Medicine, Chinese PLA General Hospital, Beijing, People's Republic of China

Lung epithelial cell apoptosis is an important feature of hyperoxia-induced lung injury. The death receptor–associated extrinsic pathway and mitochondria-associated intrinsic pathway both mediate the development of lung epithelial cell apoptosis. Despite decades of research, molecular mechanisms of hyperoxia-induced epithelial cell apoptosis remain incompletely understood. Here, we report a novel regulatory paradigm in response to hyperoxia-associated oxidative stress. Hyperoxia markedly upregulated microRNA (miR)-15a/16 levels in lung epithelial cells, bronchoalveolar lavage fluid (BALF) and lung tissue. This effect was mediated by hyperoxia-induced reactive oxygen species. Functionally, miR-15a/16 inhibitors induced caspase-3–mediated lung epithelial cell apoptosis, in the presence of hyperoxia. MiR-15a/16 inhibitors robustly enhanced FADD level and downregulated Bcl-2 expression. Consistently, cleaved caspase-8 and -9 were highly induced in the miR-15a/16–deficient cells, after hyperoxia. Using airway epithelial cell–specific, miR-15a/16$^{-/-}$ mice, we found that Bcl-2 was significantly reduced in lung epithelial cells *in vivo* after hyperoxia. In contrast, caspase-3, caspase-8 and Bcl-2–associated death promoter (BAD) were highly elevated in the miR-15a/16$^{-/-}$ epithelial cells *in vivo*. Interestingly, in lung epithelial malignant cells, rather than benign cells, deletion of *miR-15a/16* prevented apoptosis. Furthermore, deletion of miR-15a/16 in macrophages also prohibited apoptosis, which is the opposite of what we have found in normal lung epithelial cells. Taken together, our data suggested that miR-15a/16 may exert differential roles in different cell types. MiR-15a/16 deficiency results in lung epithelial cell apoptosis in response to hyperoxia, via modulating both intrinsic and extrinsic apoptosis pathways.

Online address: http://www.molmed.org
doi: 10.2119/molmed.2015.00136

INTRODUCTION

Acute lung injury (ALI) and its severe form, acute respiratory distress syndrome (ARDS), are serious clinical entities with substantial mortality and morbidity (1–3). Oxidative stress is often present in these situations, particularly in the setting of prolonged high-concentration oxygen ($FIO_2 > 0.8$) (1–3). In the past few decades, accumulating evidence demonstrates that prolonged exposure to toxic levels of oxygen causes fetal lung injury in animals (4,5). In humans, hyperoxia-induced lung injury (HALI) contributes to the development of multiple lung pathologies and also synergizes with ALI, which is caused by other factors, such as ventilator-associated overstretching and transfusion/infection-mediated pulmonary edema/inflammation (4,5). Therefore, HALI in mice has been used for decades as a model of oxidative stress mimicking clinical ARDS (6).

Hyperoxia yields reactive oxygen species (ROS) via mitochondria, including superoxide anion (O_2^-), hydrogen peroxide (H_2O_2) and hydroxyl radicals (•OH) (7,8). ROS generation leads to the damage of lipids, proteins, enzymes and nucleic acids of cells and tissues (8,9) and subsequently results in increased membrane permeability, inactivation of surfactant and inhibition of normal cellular enzyme processes. Since the 1950s, the underlying mechanisms of HALI are thought to result from ROS, which is generated directly or indirectly from high oxygen content and immune response, respectively (8–11). One of the characteristic features

Address correspondence to *Yang Jin, Pulmonary Center, Boston University Medical Campus, 72 E Concord Street, Boston, MA 02118. E-mail: yjin1@bu.edu.*
Submitted March 17, 2016; Accepted for publication April 5, 2016; Published Online (www.molmed.org) April 27, 2016.

Feinstein Institute for Medical Research
Northwell Health™

of ALI/ARDS is diffuse alveolar damage, partially contributed by alveolar epithelial cell (AEC) death, which is composed of apoptosis, necrosis and autophagic cell death (12–15). Additionally, profound vascular leak/noncardiogenic pulmonary edema, hyaline membrane production and later fibrogenesis all play important roles (14–16) in the pathogenesis of ALI/ARDS. Oxidant stress caused by hyperoxia can lead to lung epithelial cell death via multiple signaling pathways, such as the mitogen-activated protein kinase and caspase pathways (17). The caspase pathways are well characterized in modulation of apoptosis. The caspases can be activated via either the intrinsic (mitochondrial-mediated) or extrinsic (death receptor–mediated) apoptotic pathways (18–20). The intrinsic apoptotic pathway features mitochondrial release of cytochrome c and initiates activation of the caspase cascade through caspase-9. This pathway also involves Bcl-2 proteins. The extrinsic apoptotic pathway is activated by death receptors on the plasma membrane, such as Fas/CD95, subsequently forming the death-inducing signaling complex involving FADD and initiating the caspase cascade through caspase-8 (18–20).

Despite decades of extensive research, ROS is still thought of as the main culprit for hyperoxia/oxidative stress–induced lung epithelial cell death. In this report, we investigated a novel paradigm in the pathogenesis of hyperoxia-induced lung epithelial death. We found that microRNAs (miRNAs, abbreviated miR) induced by hyperoxia-derived ROS modulated multiple pathways involved in apoptosis in lung epithelial cells. Here we focus on exploring the effects of miR-15a/16 on hyperoxia-induced lung epithelial cell death.

MiR-15a and 16 both belong to the miR-15 miRNA precursor family (21–23). MiRNAs refer to small noncoding RNA genes that play crucial roles in regulating gene expression. The miR-15 miRNA precursor family includes the related miR-15a, 15b, 16-1, 16-2, 195 and 497 (21–23). In humans, *miR-15a* and *miR-16* are clustered within 0.5 kb at chromosome 13q14 (21–23) and are commonly deleted together during the generation of knockout mice. Bcl-2 has been reported as one of the targets of miR-15a/16. So far, miR-15a and 16 have been thought to be involved in tumor biology, particularly in chronic lymphocytic leukemia (21–23). To the best of our knowledge, this is the first report to link miR-15a/16 to the regulation of lung epithelial cell death. Our research sheds light on the pathogenesis of hyperoxia-induced cell death and lung injury.

MATERIALS AND METHODS

Reagents and Chemicals

N-Acetyl cysteine (NAC), H_2O_2, MISSION Synthetic human negative control miRNA (NCSTUD001), human hsa-miR-15a-5p inhibitor (HSTUD0256), human hsa-miR-16-5p inhibitor (HSTUD0260), human hsa-miR-15a mimic (HMI0256) and human hsa-miR-16 mimic (HMI0262) were purchased from Sigma-Aldrich. All antibodies for Western blot analysis were purchased from Cell Signaling Technology.

Animals

C57BL/6J mice and stock loxP-miR 15a/16$^{-/-}$ mice were purchased from the Jackson Laboratory. Cre-lox technology was used to generate cell-specific miR15a/16 knockout mice to ensure that gene function could be studied in specific cells. Cre-CC10-miR15a/16$^{-/-}$ hybrids and control mice Cre-CC10 wild-type (WT) hybrids were used to study miRNA functions in lung epithelial cells. Myeloid-specific Cre mice were purchased from the Jackson Laboratory and crossbred to generate myeloid-specific miR-15a/16$^{-/-}$ Cre mice. All mice were housed according to the guidelines of the American Association for Laboratory Animal Care 2011/ Eighth Edition (24). Animal protocols were approved by the Animal Research Committee of Brigham and Women's Hospital. Mice (8 wks old, male, weight: 19.7 ± 1.2 g) were placed in a Plexiglas chamber maintained at 100% O_2 (hyperoxia group) or in a chamber open to room air (RA; normoxic group).

Cell Culture

Beas2B cells (ATCC) were cultured in Dulbecco's modified Eagle's medium (DMEM) with 10% fetal bovine serum (FBS). All cells were grown at 37°C in a humidified atmosphere of 5% CO_2. For the hyperoxia group, cells were exposed to hyperoxia (95% oxygen with 5% CO_2) in modular exposure chambers as previously described (25).

Beas2B cells were seeded in 6-cm dishes, grown to about 70% confluence and then used for cell transfection. For each dish, 1.5 μg of miRNA (negative control, miRNA mimic or miRNA inhibitor) was added to siRNA Transfection Medium. Ten microliters of INTERFERin (Polyplus) was added to the siRNA duplexes per the manufacturer's protocol. After 12 h, cells were exposed to hyperoxia or RA for another 24 h according to the experimental protocol.

AEC Isolation

Primary mouse lung epithelial cells were isolated as previously described (25). Briefly, antibody-coated plates were prepared 1 d before isolation: including 5 mL of PBS, 82 μL of anti-CD45 antibody (BD Biosciences #553076) and 32 μL of anti-CD16/32 antibody (BD Biosciences #553142). A 10-cm cell culture dish was used for each mouse. These plates were incubated at 4°C for 24 h. Mice were euthanized, and their thoracic cages were exposed. Lungs were perfused with cold PBS via the right ventricle (RV) of the heart until free of blood, followed by 2 mL of dispase (Stem Cell Technologies), which was instilled rapidly. Lung primary cells were isolated in the culture hood. Cell mix was filtered using 100-, 40- and 20-μm cell strainers sequentially. Cells were then centrifuged at 300 *g* for 10 min at 4°C. After centrifugation, the cells were resuspended in 5 mL of DMEM (437.5 mL

DMEM + 12.5 mL 1 mol/L HEPES + 50 mL FBS) and transferred to the antibody-coated plate. After incubation, cells were gently rinsed off the plate and centrifuged at 300 *g* for 10 min at 4°C. The supernatant was discarded, and cells were resuspended in 7 mL of DMEM. The cell suspension was inoculated into a noncoated culture plate for 4 h in a cell culture incubator. After incubation, all the cells were collected, rinsed and centrifuged at 300 *g* for 10 min at 4°C. Cells were then transferred to 6-mm cell culture dish and cultured in DMEM. After 60 h, the cells were used for further experiments.

Real-Time Polymerase Chain Reaction

Total RNA was extracted using miRNeasy Mini Kit (Qiagen). Complementary DNA was synthesized using 2 μg of total RNA per sample with ABI mRNA Reverse Transcription Kit (Applied Biosystems), according to the manufacturer's protocol. The primers (TaqMan Gene Expression Assays) were bought from Applied Biosystems (miR-15a: mm04238182_S1, Hs04231417_S1; miR-16: mm04238183_S1, Hs04231418_S1; HPRT: mm00446968_m1, Hs99999909_m1; ATG5: Hs00169468_m1; ATG7: Hs00197348_m1; ATG12: Hs00740818_m1; GAPDH: Hs03929097_g1). Quantitative real-time polymerase chain reaction (PCR) was performed in triplicate for each sample using the TaqMan Probe-Based Gene Expression Analysis on a 7300 Real-Time PCR System (Applied Biosystems) at the recommended thermal cycling settings: one initial cycle at 95°C for 10 s, followed by 40 cycles at 95°C for 5 s and 60°C for 30 s.

Western Blot Analysis

Cells were harvested after washing twice with cold PBS and then suspended in radioimmunoprecipitation assay buffer with protease inhibitors (Roche) and phosphatase inhibitor (Roche). Equal amounts of proteins were subjected to sodium dodecyl sulfide-polyacrylamide gel electrophoresis and transferred to polyvinylidene fluoride (PVDF) membranes. The PVDF membrane was blocked with 5% nonfat milk and incubated overnight at 4°C with 1:1000 monoclonal antibodies. Then, the PVDF membrane was incubated with a horseradish peroxidase-linked secondary antibody (1:2000) for 1 h at room temperature. Immunoreactive bands were visualized using luminol reagent.

Immunohistochemistry

Bcl-2 antibody (sc-492) was obtained from Santa Cruz. Caspase-3 antibody (ab4501) was from Abcam. Caspase-8 antibody (9496) was from Cell Signaling Technology. The VECTASTAIN ELITE ABC Kit and Peroxidase Substrate Solution Kit (DAB) were purchased from Vector Laboratories. Tissue sections were deparaffinized and hydrated through xylenes and graded alcohol series, followed by incubation with primary antibodies, washing and dilution with biotinylated secondary antibody solution. Sections were developed with VECTASTAIN ABC reagent, per the manufacturer's protocol.

Measurement of Cell Apoptosis Using Flow Cytometry

Annexin V-FITC Plus Assay (BioVision) was used to analyze cell apoptosis. Beas2B cells were harvested and resuspended in PBS with Annexin V-FITC and SYTOX Green dye. After 10-min incubation, cell apoptosis was analyzed using BD FACS Canto II and FlowJo software (Ashland).

Terminal Deoxynucleotidyl Transferase dUTP Nick-End Labeling Assays

Beas2B cells were cultured on sterile glass coverslips. Next, cells were transfected with miRNA inhibitors, followed by hyperoxia exposure. TACS·XL-Blue Label *In Situ* Apoptosis Detection Kit (Trevigen) was used for cell apoptosis detection. Cells were examined under a microscope. Cells with DNA fragmentation were stained in an intense blue color, while normal cells were in pale red counterstain, per the manufacturer's protocol.

Cell Viability Assay

The CellTiter-Glo Luminescent Cell Viability Assay (Promega) was used to assess the cell viability. The cells were seeded in 96-well plates. When grown to about 70% confluence, they were transfected by miR-15a/16 inhibitors or negative control miRNA and then administered by RA or hyperoxia. At the time point we set, 100 μL of the CellTiter-Glo reagent was added directly into each well for 10-min incubation. The plates were read by GloMax 96 microplate luminometer (Promega).

Caspase Activity Assay

Cells were seeded into 96-well plates at a density of 8,000 cells/well. Blank reaction wells (Caspase-Glo 3/7 reagent, cell culture medium without cells), negative control cells (Caspase-Glo 3/7 reagent, cells without any treatment) and assayed cells (treated with inhibitors or from primary cell) were set up. The Caspase-Glo 3/7 Assay was purchased from Promega, and assays were performed according to the manufacturer's protocol. Briefly, 100 μL of Caspase-Glo 3/7 reagent was added to each well of a white-walled 96-well plate containing 100 μL of blank, negative control cells or treated cells in culture medium, respectively. After gentle mix and incubation at room temperature for 45 min, the luminescence of each sample as relative light units was obtained using a plate-reading luminometer.

Statistical Analysis

All data were presented as mean ± standard deviation, and all experiments were repeated at least three times. Statistical analyses were performed using GraphPad Prism 5 (GraphPad Software). The Student *t* test and one-way analysis of variance with Tukey method were applied for analysis. P values of <0.05 were considered significant.

All supplementary materials are available online at www.molmed.org.

RESULTS

Hyperoxia Rapidly Induces miR-15a/16 Generation in Lung Epithelial Cells, and This Effect Is ROS Dependent

Initially, we found that miR-15a and 16 were highly induced by hyperoxia in Beas2B human lung epithelial cells (Figure 1A). Upregulation of miR-15a and 16 peaked approximately 12 h after exposure to hyperoxia (Figure 1A). This observation prompted us to investigate whether hyperoxia also induces miR-15a and 16 *in vivo*. C57BL/6 mice were exposed to hyperoxia (100%) as previously described (25). Consistently, hyperoxia induced miR-15a and 16 expression in mouse lung tissue in a time-dependent manner (Figure 1B). We next evaluated miR-15a/16 levels in BALF. As shown in Figure 1C, hyperoxia upregulated the release of miR-15a/16 in BALF. To determine whether hyperoxia induced miR-15a/16 via ROS, we treated Beas2B epithelial cells with H_2O_2, a known ROS donor. Multiple previous reports have established the concepts that H_2O_2 is a strong inducer of ROS production in the lung epithelial cell systems that we are using (26). Robust induction of miR-15a/16 was identified in Beas2B cells (Figure 1D). H_2O_2 is an established ROS generator (27). However, as a strong ROS generator, it can cause significant cell death and commonly only short-term exposure is used (28; Supplementary Figure S4). Promisingly, with only 4-h exposure, H_2O_2 had already induced miR-15a/16 significantly (Figure 1E). Moreover, induction of miR-15a/16 by hyperoxia was blunted when Beas2B cells were pretreated with the ROS scavenger, NAC (Figure 1F). NAC is a well-known suppressor of ROS generation in lung epithelial cells (29). These results indicate that hyperoxia induces miR-15a/16 expression in lung epithelial cells via ROS generation.

MiR-15a/16 Inhibitors Promote Hyperoxia-Induced Apoptosis in Lung Epithelial Cells

To examine the functional roles of miR-15a and 16, we transfected the Beas2B cells with inhibitor control, miR-15a or 16 inhibitors, followed by RA or hyperoxia exposure. Given that in the presence of hyperoxia, the endogenous miR-15a/16 level had significantly increased rather than decreased (Figure 1), we chose to use the "loss of function" approach by suppressing miR-15a/16 using inhibitors or knockouts, rather than overexpressing it using mimics. We found that miR-15a or 16 inhibitors promoted apoptosis in Beas2B cells, in the presence of hyperoxia (Figure 2A, B). To further confirm our observations, we generated airway epithelial cell–specific miR-15a/16–deficient mice, Cre-CC10-miR-15a/16$^{-/-}$ mice. We next isolated the primary lung epithelial cells from Cre-CC10-miR-15a/16$^{-/-}$ mice and cultured them as previously described (25). After exposure to hyperoxia, primary epithelial cells isolated from miR-15a/16$^{-/-}$ mice showed higher apoptosis compared with the epithelial cells isolated from control mice (Figure 2C).

MiR-15a/16 Inhibitors Promote Apoptosis in Lung Epithelial Cells via Both Intrinsic and Extrinsic Pathways

In epithelial cells, both intrinsic and extrinsic apoptotic pathways have been reported in the presence of hyperoxia (18–20,30,31). To further confirm the above observations and delineate the underlying mechanisms, we determined the effects of miR-15a/16 deficiency on the regulatory proteins involved in these apoptotic pathways. Caspase-3 is the ultimate checkpoint at the common apoptotic pathway, where both intrinsic and extrinsic pathways convene (18–20). We found that miR-15a or 16 inhibitors increased caspase-3 activity significantly (Figure 3A). Consistently, higher levels of caspase-3 were also detected in Beas2B cells that were transfected with miR-15a/16 inhibitors (Figure 3B). The cleaved caspase-8 and FADD were robustly increased after hyperoxia in these miR-15a/16-deficient Beas2B cells (Figure 4A, B), suggesting that extrinsic pathways were involved in this process (Figure 4A, B). Furthermore, miR-15a/16 deficiency downregulated Bcl-2 and upregulated cleaved caspase-9 in Beas2B cells (Figure 4C, D). This observation indicated that the intrinsic apoptotic pathways were also involved in the miR-15a/16 deficiency–related apoptosis. Bik and p-Bad, pro-apoptosis proteins, were elevated after miR-15a/16 inhibition (Supplementary Figure S1C). However, inhibitors of miR-15a/16 failed to alter the levels of SMAC, survivin, FLIP, Bcl-xL, Mcl-1, Bak, Bim, Puma and Bax, suggesting that miR-15a/16 have specific targets instead of universally affecting all apoptosis regulators (Supplementary Figure S1).

We next confirmed the effects of miR-15a/16 deficiency on lung epithelial cell apoptosis using Cre-CC10-miR-15a/16$^{-/-}$ mice *in vivo*. After exposure to hyperoxia (3 d), immunohistochemistry (IHC) was performed using the lung sections obtained from these mice. Caspase-3, caspase-8 and BAD were highly elevated in the miR-15a/16$^{-/-}$ epithelial cells *in vivo* (Figure 5B, C, D). In contrast, Bcl-2 was decreased (Figure 5A). We next isolated the primary lung epithelial cells from the Cre-CC10-miR-15a/16$^{-/-}$ mice. Cells from the Cre-CC10-miR-15a/16$^{-/-}$ mice had lower survival compared with the control cells (Supplementary Figure S5). These data were consistent with our observations using miR-15a/16 inhibitors in Beas2B cells.

Hyperoxia also induced miR-15a/16 generation in macrophages and A549 (Supplementary Figures S2A and S3A). To determine the effects of miR-15a/16 deficiency on macrophage and tumor cell apoptosis, we isolated bone marrow–derived macrophages from the mononuclear cell–specific Cre-miR-15a/16$^{-/-}$ mice. As shown in Supplementary Figure S2B, unlike the situation in epithelial cells, deletion of miR-15a/16 resulted in higher survival. Furthermore, miR-15a/16 inhibitors increased survival in A549 cells, while the miR-15a/16 mimics decreased survival. This observation was opposite of the effects of miR-15a/16 in normal lung epithelial cells. These data were consistent

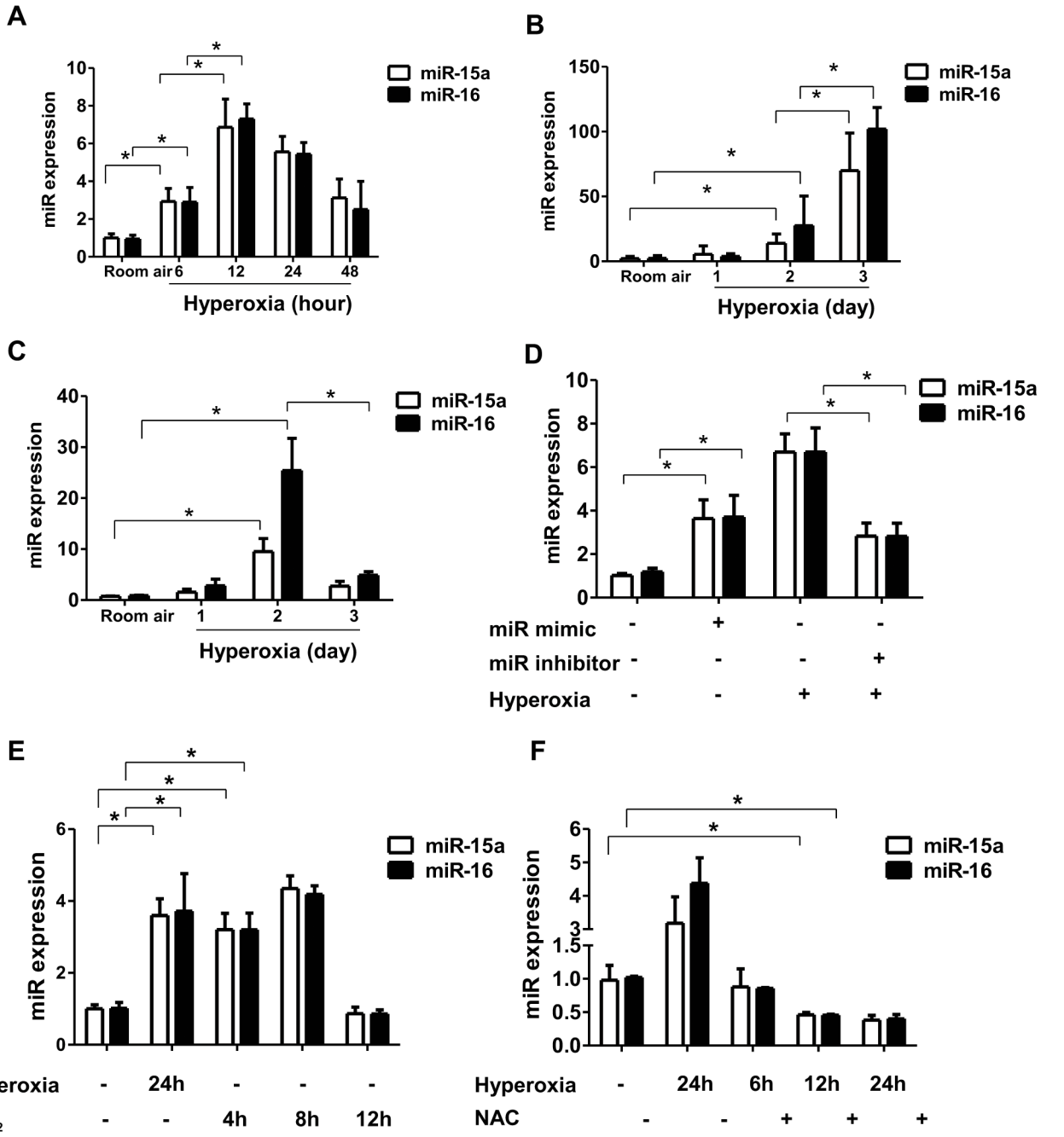

Figure 1. Effects of hyperoxia on miR-15a/16 levels. (A) Beas2B cells were exposed to room air (RA) or hyperoxia (95% O_2, 5% CO_2) for a time course between 6 and 48 h. miRNA was analyzed using real-time PCR. Figures represent three independent experiments with similar results. *$p < 0.05$. (B) C57BL/6J mice were exposed to RA or hyperoxia (100%). After 1–3 d, lung tissue miRNA was isolated and analyzed using real-time PCR (mean ± standard deviation (SD), n = 10). *$p < 0.05$. (C) C57BL/6J mice were exposed to RA or hyperoxia (100%). After 1–3 d, BALF miRNA was analyzed using real-time PCR (mean ± SD, n = 10). PCR (mean ± SD, n = 10). *$p < 0.05$. (D) Beas2B cells were incubated with RA, H_2O_2 (100 μmol/L), hyperoxia (95% O_2, 5% CO_2) or H_2O_2 (100 μmol/L) + hyperoxia (95% O_2, 5% CO_2). After 6 h, miRNA was analyzed using real-time PCR. Figures represent three independent experiments with similar results. *$p < 0.05$. (E) Beas2B cells were incubated with RA, H_2O_2 (40 μmol/L) or hyperoxia (95% O_2, 5% CO_2). After a designated time point, miRNA was analyzed using real-time PCR (mean ± SD, n = 3). *$p < 0.05$. (F) Beas2B cells were exposed to RA or hyperoxia (95% O_2, 5% CO_2) in the absence or presence of NAC (5 mmol/L). After 6 h, miRNA was analyzed using real-time PCR. Figures represent three independent experiments with similar results. *$p < 0.05$.

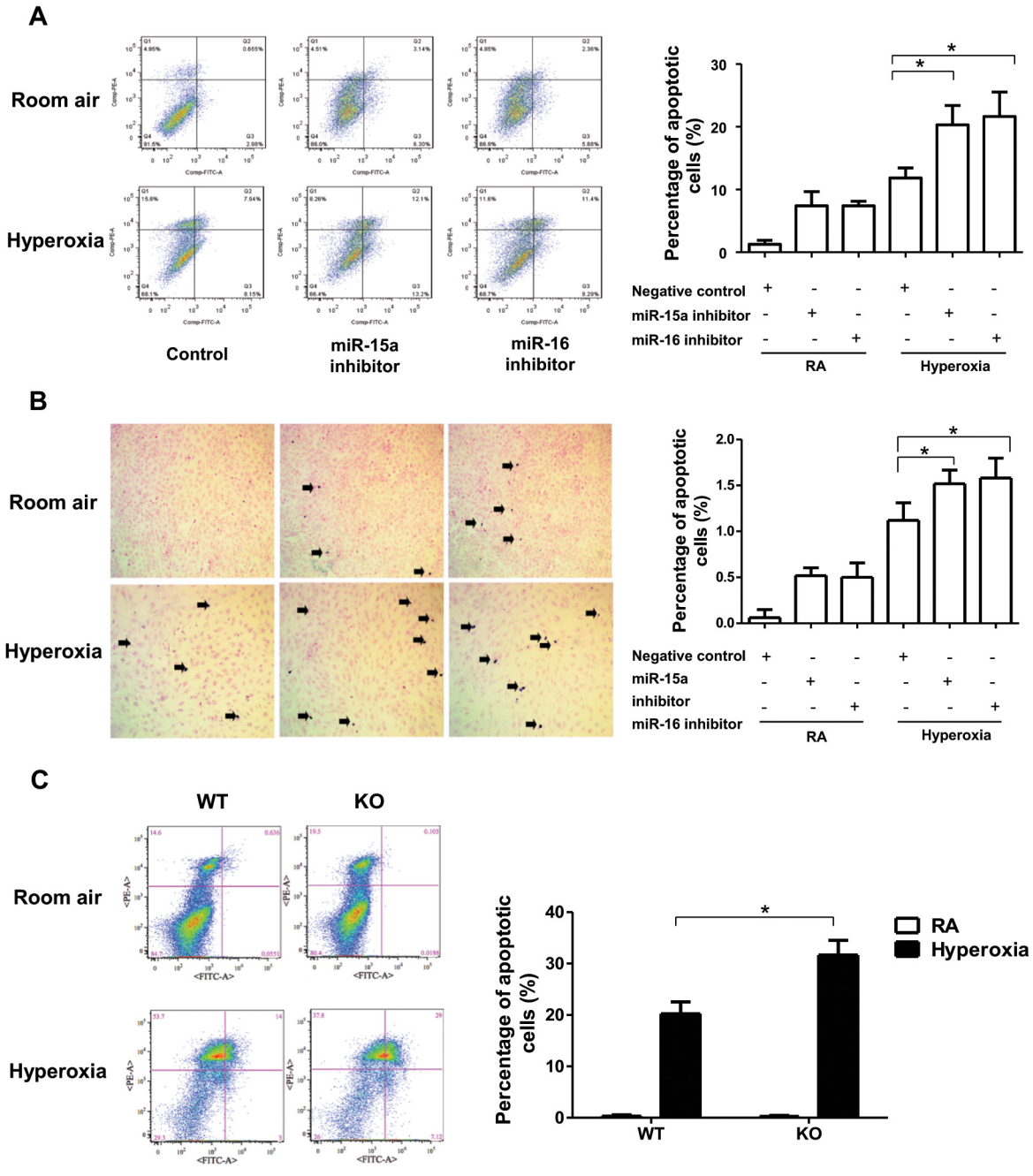

Figure 2. Suppression of miR-15a/16-induced apoptosis after hyperoxia. Beas2B cells were grown to approximately 70% confluence and transfected with negative controls or miR-15a/16 inhibitors. After 12 h, the cells were exposed to RA or hyperoxia (95% oxygen). After another 24 h, the cells were harvested for flow cytometry analysis (A) or terminal deoxynucleotidyl transferase dUTP nick-end labeling (TUNEL) staining (B). (A) Apoptosis of Beas2B cells was analyzed using flow cytometry. Statistical analysis is shown on the right. Figures represent three independent experiments with similar results. *$p < 0.05$. (B) TUNEL staining of Beas2B cells after hyperoxia. Apoptotic nuclei were labeled by TUNEL (black arrow). Statistical analysis is shown on the right. Figures represent three independent experiments with similar results. *$p < 0.05$. (C) AECs were isolated from hybrid mice (mice after crossbreeding C57BL/6J WT mice with CC10 Cre mice serve as control; mice after crossbreeding miR15a/16$^{-/-}$ loxP mice with CC10 Cre mice serve as lung epithelial cell–specific miR-15a/16$^{-/-}$ mice). AEC were cultured for 6 d and then were incubated in room air (RA) (21% oxygen) or hyperoxia (95% oxygen) for 24 h. Next, the cells were harvested and detected using FACS. Statistical analysis is shown on the right. Figures represent two independent experiments with the similar results. *$p < 0.05$.

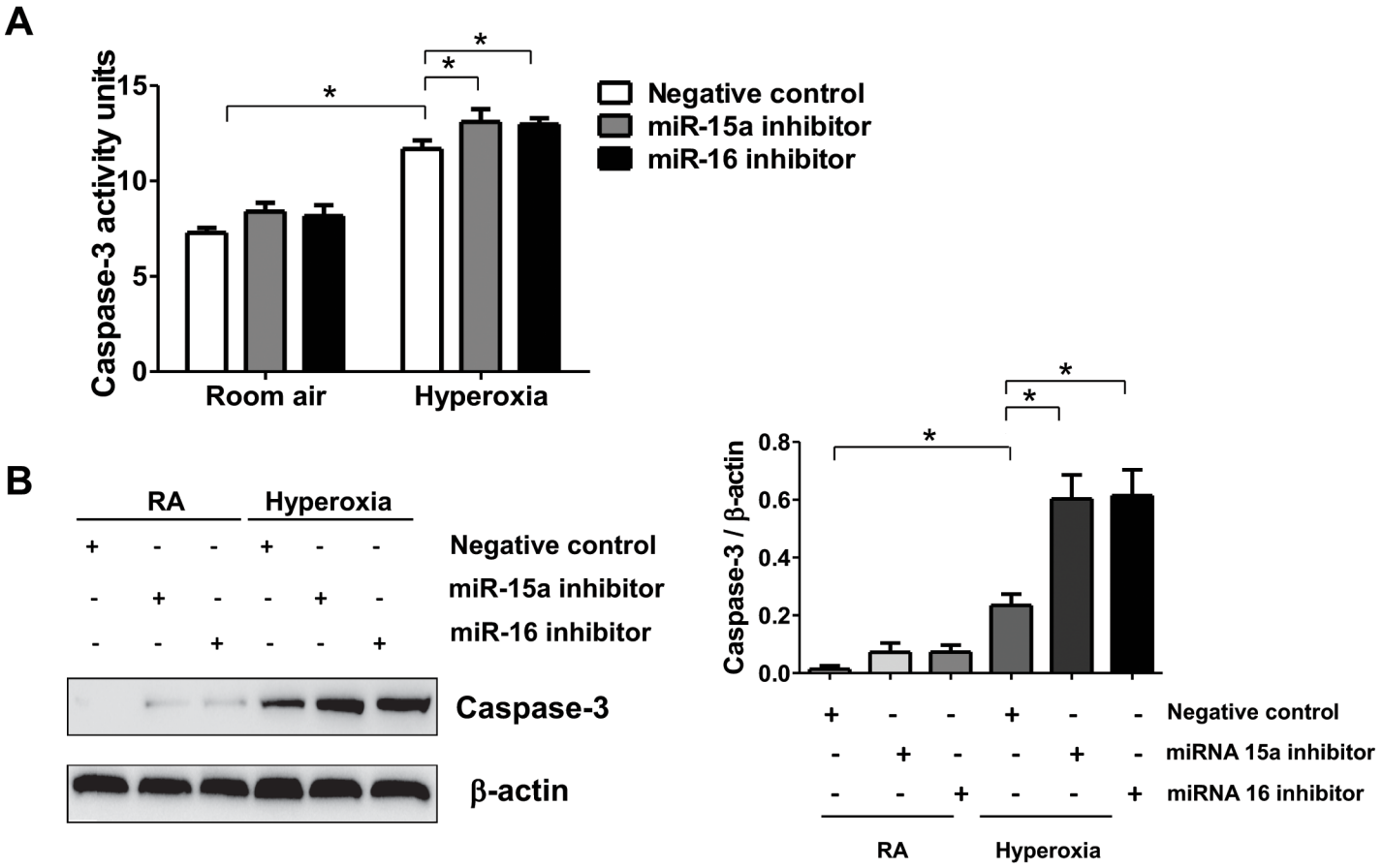

Figure 3. Suppression of miR-15a/16 induced apoptosis via caspase-mediated pathways. (A) Beas2B cells were transfected with miR-15a/16 inhibitors or negative controls. After hyperoxia (2 d), caspase-3 activity was determined. Figures represent three independent experiments with similar results. *$p < 0.05$. (B) Beas2B cells were transfected with miR-15a/16 inhibitors or negative controls. After hyperoxia (1 d), caspase-3 was detected using Western blot analysis. Statistical analysis is shown on the right. Figures represent three independent experiments with similar results. *$p < 0.05$.

with previous reports using immunomodulatory cells or tumor cells (32,33)

DISCUSSION

MiRNAs have emerged as important regulators of essential cellular processes, such as cell death, growth and survival (21–23,32,33). Expression of tissue-specific miRNAs in response to stress stimuli often directly regulates the genes that determine the ultimate fate of these tissue cells (21–23,32,33). This observation has been repeatedly reported in cancer research. However, roles of miRNAs in the death and survival of normal lung epithelial cells in response to oxidative stress remain unclear.

Based on our previous observations, miR-15a/16 is not only highly expressed in the lungs, but also can be found in circulating serum (34). Therefore, we chose miR-15a/16, a potential candidate for biomarker development, to further explore its biological functions. Our studies showed that miR-15a/16 inhibitors promoted lung epithelial cell apoptosis in response to hyperoxic stress, a common factor involved in the development of ALI. We have noted that the inhibition of miR-15a or 16 indeed caused a certain degree of apoptosis in both RA and hyperoxic conditions. However, as shown in Figure C, when using the miR-15a/16 dual-knockout cells, a synergistic effect, rather than an additive effect, had been demonstrated.

Hyperoxia-associated oxidative stress rapidly upregulated miR-15a/16 levels in airway epithelial cells, lung tissue and BALF (Figure 1). This transient upregulation of miR-15a/16 in nontumor epithelial cells subsided with prolonged exposure to hyperoxia (Figure 1). The abruptly elevated miR-15a/16 may reflect an innate response in attempting to salvage the cells from undergoing apoptosis. As shown in our data, miR-15a/16 inhibitors led to propagated apoptosis via modulation of both the intrinsic and extrinsic apoptotic pathways (Figure 6). Similarly, miR-15a/16 has been reported

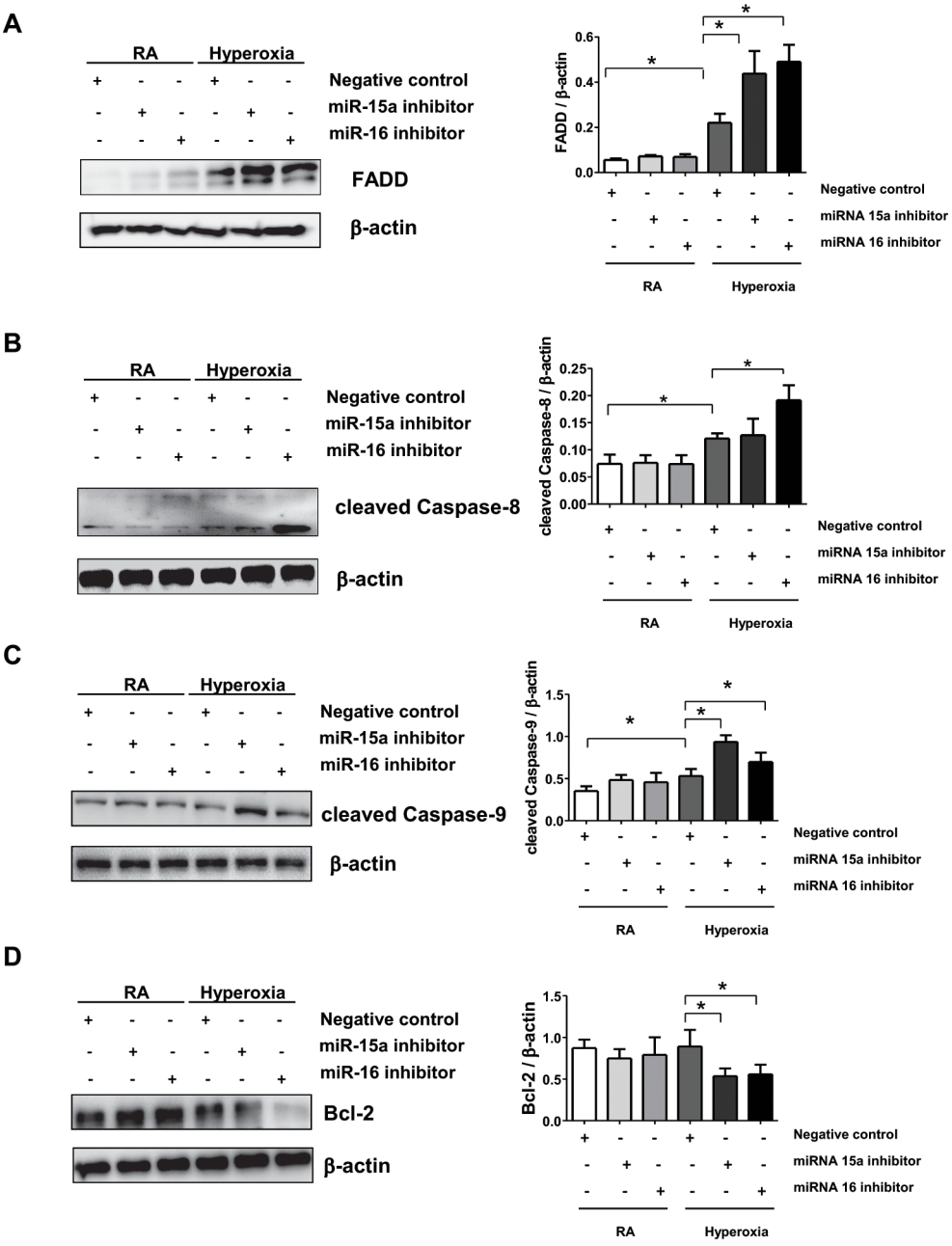

Figure 4. Suppression of miR-15a/16 modulated both intrinsic and extrinsic pathways. As above, Beas2B cells were transfected with miR-15a/16 inhibitors or negative controls. Western blot analysis was used to determine the protein level. (A) FADD; (B) cleaved caspase-8; (C) Bcl-2; (D) cleaved caspase-9. Statistical analysis is shown on the right. Figures represent three independent experiments with similar results. *$p < 0.05$.

to modulate both the intrinsic and extrinsic apoptosis pathways (35,36). Based on our previous work, both intrinsic and extrinsic pathways are involved in the final fate of lung epithelial cells (11). However, there has not been a quantitative method to determine the extent to which these individual pathways are contributing to apoptosis.

MiR-15a and 16 belong to the miR-15 miRNA precursor family (21–23,32,33). The miR-15 miRNA precursor family includes the related miR-15a and 15b, miR-16-1 and 16-2, miR-195, and miR-497 (21–23). *MiR-15a* and *MiR-16* are clustered within 0.5 kb at chromosome position 13q14 in humans (21–23). Interestingly, in contrast to our observations in normal

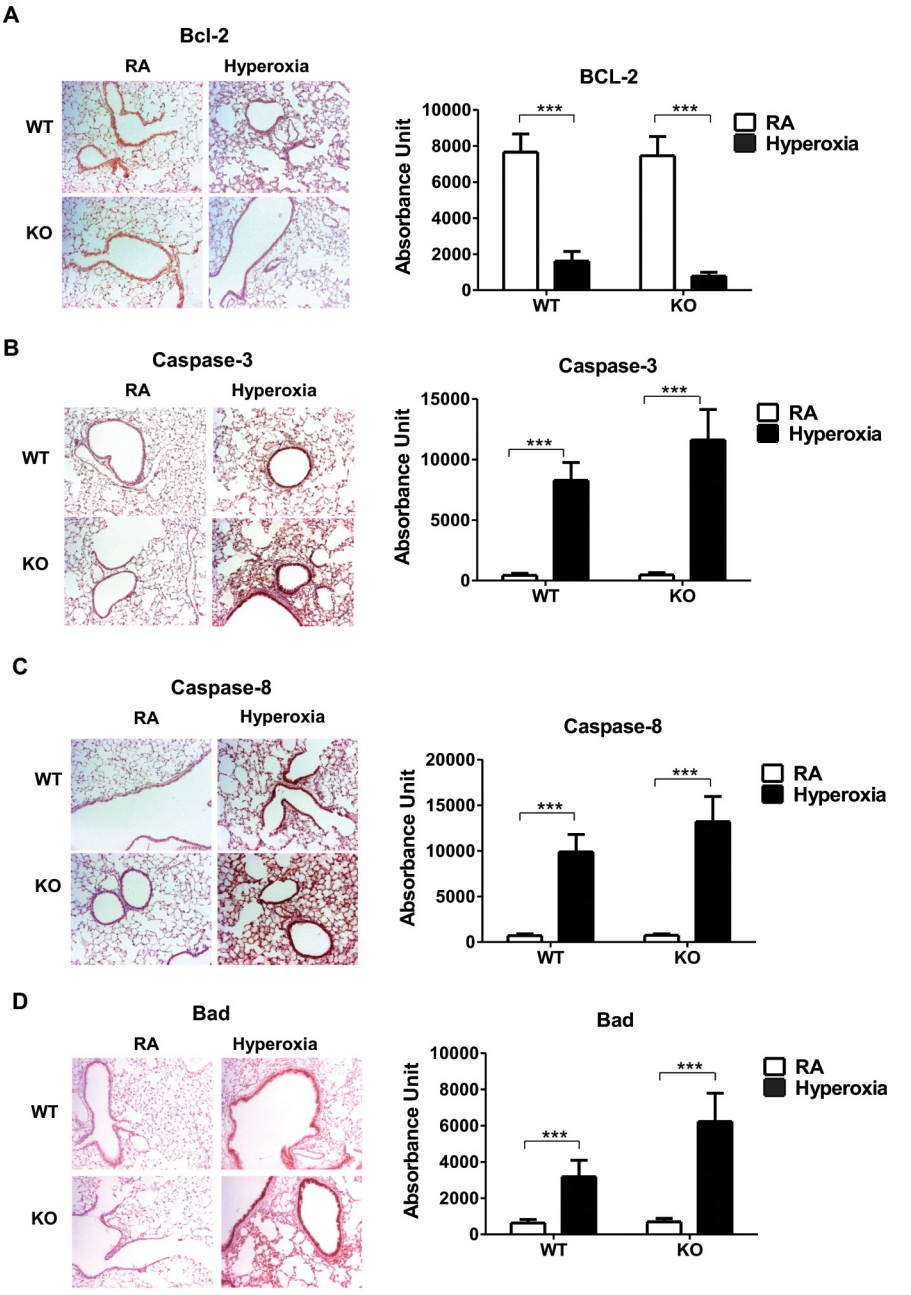

Figure 5. Suppression of miR-15a/16 modulated both intrinsic and extrinsic pathways, detected using IHC *in vivo*. Lung epithelial cell–specific miR-15a/16$^{-/-}$ mice and control mice (described in Figure 2 legend) were exposed to hyperoxia (right panels in the figures) or room air (RA; left panels in the figures). After 3 d, lung tissue sections were obtained. Bcl-2, caspase-3, caspase-8 and Bad were detected using IHC staining. Positive cells were stained with DAB (×200). Statistical analysis is shown on the right. Figures represent two independent experiments with similar results. *$p < 0.05$.

lung epithelial cells, miR-15a/16 deficiency promoted cell survival in lung tumor cells and macrophages (Supplementary Figures S2 and S3).

Consistently, previous reports have showed that deletion of *miR-15a/16-1* accelerates the proliferation of both human and mouse B cells via regulating cell cycle–associated genes (21–23,32,33). Previous reports have also demonstrated that the miR-15a/16-1 miRNA cluster functions as a tumor suppressor, targeting Bcl-2 protein in prostate tumor cells (21–23,32,33). Inhibition of cell proliferation by miR-15a/16-1 has been reported to occur in both lymphoid and nonlymphoid tissue (21–23,32,33,37,38), Wang *et al*. (40) further demonstrated the miR-15a level is increased and it induces cell death in an ischemia reperfusion model (39,41). Our current studies revealed a differential effect of miR-15a/16 on apoptosis in nontumor lung epithelial cells. Our data suggest that miR-15a/16 in fact may function as a homeostatic factor, which balances cell death and survival, depending on the specific cell types and conditions.

Like all other miRNAs, miR-15a/16 has a broad range of cellular targets. Our results further demonstrated that miR-15a/16 differentially regulated a target gene based on the specific stimulation. For example, deletion of miR-15a/16 upregulates Bcl-2 in tumor cells (22,23). In our studies using nontumor epithelial cells, miR-15a/16 inhibitors negatively regulate Bcl-2, but positively regulate FADD and caspases after hyperoxia (Figures 3, 4, 5). All these differential results of miR-15a/16 function further indicate that miR-15a/16 exerts differential cellular functions in different cell types, upon receiving specific stimuli.

We found that miR-15a/16 can be secreted from cells and detected in serum (34). Although hyperoxia induced miR-15a/16 expression, using transfected mimics or inhibitors, we only explored the *in vitro* functions of miR-15a/16. Therefore, this work probably reflects more on the functions of intracellular miR-15a/16. After hyperoxia, the miR-15a/16 released from cells potentially had no effects on the fate of Beas2B cells themselves. We speculate that the Beas2B-secreted miR-15a/16 has potential vital functions on the adjacent cells in the microenvironment of lung parenchyma. However, this requires further investigation.

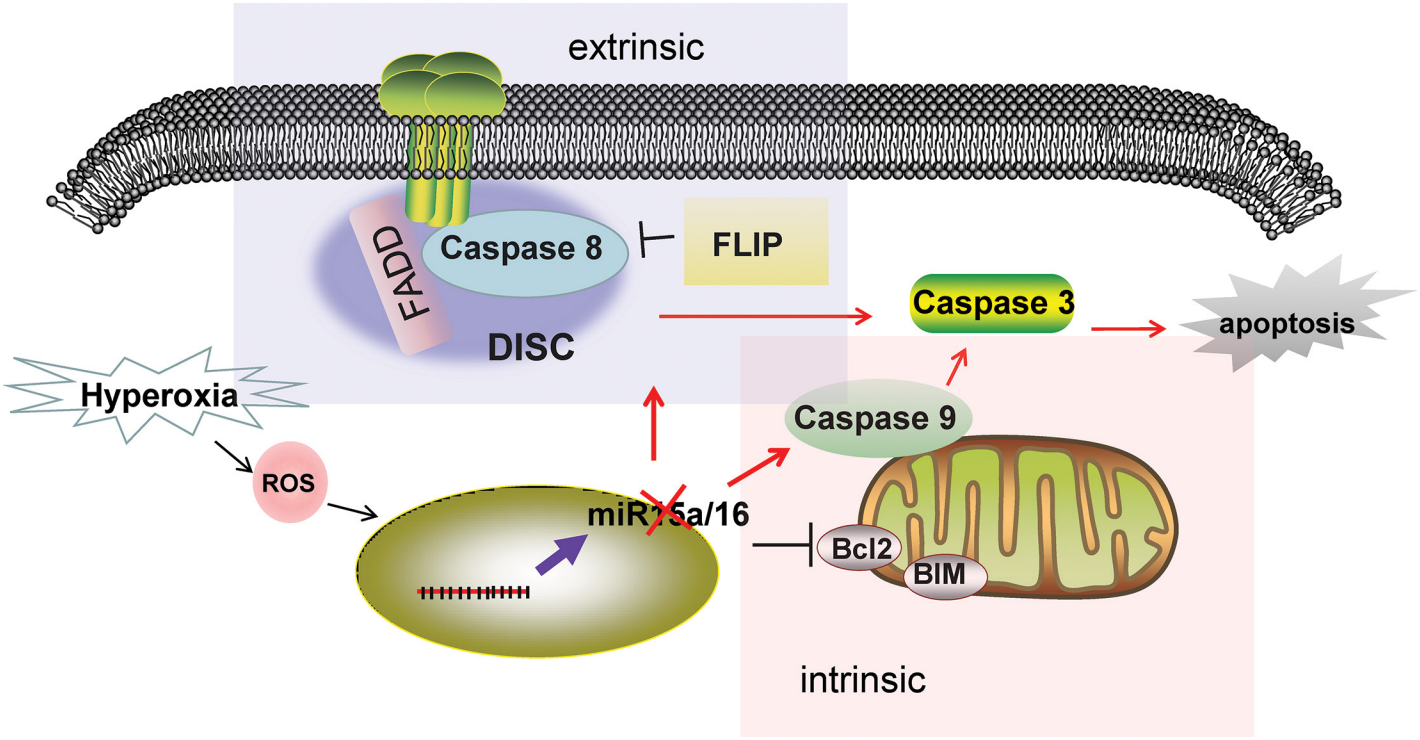

Figure 6. Suppression of miR-15a/16 promoted apoptosis in lung epithelial cells via both intrinsic and extrinsic pathways (schema). Hyperoxia induced miR-15a/16 expression in lung epithelial cells via ROS generation. Suppression of miR-15a/16 promoted FADD/caspase-8–associated DISC formation. On the other hand, miR-15a/16 deficiency activated caspase-9 via decreased Bcl-2. Thus, suppression of miR-15a/16 promoted caspases-mediated apoptosis in lung epithelial cells, in response to hyperoxia.

MiR-15a/16 also targets cell cycle regulators. Inhibition of miR-15 expression enhances cyclin E1 mRNA and protein levels (41). Inhibition of both miR-15 and 16 expression augments G_1/S transition, while overexpression of miR-15 reduces cyclin E protein levels and inhibits the G_1/S transition (42). Our future work will explore the effects of miR-15a/16 on cell cycle regulators after hyperoxia and further characterize the roles of miR-15a/16 in lung epithelial cell homeostasis in response to oxidative stress. Additionally, future studies are needed to address the functions of both intracellular and extracellular miR-15a/16 in the pathogenesis of lung diseases.

CONCLUSION

Our studies illustrated that miR-15a/16 targeted the regulatory proteins, which involved both intrinsic and extrinsic apoptotic pathways. MiR-15a/16 potentially serves as an important factor regulating cellular homeostasis.

ACKNOWLEDGMENTS

This work is supported by the National Institutes of Health (R01 HL102076 and R01 GM111313 to YJ). We thank Mr. Jincheng Yang for his assistance on hyperoxia-related studies.

DISCLOSURE

The authors declare they have no competing interests as defined by *Molecular Medicine*, or other interests that might be perceived to influence the results and discussion reported in this paper.

REFERENCES

1. Bernard GR. (2005) Acute respiratory distress syndrome: a historical perspective. *Am. J. Respir. Crit. Care Med.* 172:798–806.
2. Rubenfeld, *et al.* (2005) Incidence and outcomes of acute lung injury. *N. Engl. J. Med.* 353:1685–93.
3. Lee PJ, *et al.* (1996) Regulation of heme oxygenase-1 expression in vivo and in vitro in hyperoxic lung injury. *Am. J. Respir. Cell Mol. Biol.* 14: 556–68.
4. Kallet RH, Matthay MA. (2003) Hyperoxic acute lung injury. *Respir. Care.* 58:123–41.
5. Mantell LL, Lee PJ. (2000) Signal transduction pathways in hyperoxia-induced lung cell death. *Mol. Genet. Metab.* 71:359–70.
6. Matute-Bello G, Frevert CW, Martin TR. (2008) Animal models of acute lung injury. *Am. J. Physiol. Lung Cell. Mol. Physiol.* 295: L379–L99.
7. Zaher TE, Miller EJ, Morrow DM, Javdan M, Mantell LL. (2007) Hyperoxia-induced signal transduction pathways in pulmonary epithelial cells. *Free Radic. Biol. Med.* 42:897–908.
8. Devasagayam TP, *et al.* (2004) Free radicals and antioxidants in human health: Current status and future prospects. *J. Assoc. Physicians India.* 52:794–804.
9. Martindale JL, Holbrook NJ. (2002) Cellular response to oxidative stress: signaling for suicide and survival. *J. Cell Physiol.* 192:1–15.
10. Conner GE, Salathe M, Forteza R. (2002) Lactoperoxidase and hydrogen peroxide metabolism in the airway. *Am. J. Respir. Crit. Care Med.* 166: S57–S61.

11. Zhang M, *et al.* (2011) Caveolin-1 mediates Fas-BID signaling in hyperoxia-induced apoptosis. *Free Radic. Biol. Med.* 50:1252–62.
12. Cotran RS, *et al.* (2005) *Robbins and Cotran Pathologic Basis of Disease*. St. Louis (MO): Elsevier Saunders, p. 715.
13. Parambil JG, Myers JL, Ryu JH. (2006) Diffuse alveolar damage: Uncommon manifestation of pulmonary involvement in patients with connective tissue diseases. *Chest.* 130:553–8.
14. Ryter SW, Choi AM. (2010) Autophagy in the lung. *Proc. Am. Thorac. Soc.* 7:13–21.
15. Parambil JG, Myers JL, Aubry MC, Ryu JH. (2007) Causes and prognosis of diffuse alveolar damage diagnosed on surgical lung biopsy. *Chest.* 132:50–7.
16. Jin Y, Tanaka A, Choi AM, Ryter SW. (2002) Autophagic proteins: New facets of the oxygen paradox. *Autophagy.* 8:426–8.
17. Li X, Shu R, Filippatos G, Uhal BD. (2004) Apoptosis in lung injury and remodeling. *J. Appl. Physiol.* 97:1535–42.
18. Savill J, Gregory C, Haslett C. (2003) Eat me or die. *Science* 302:1516–17.
19. Taylor RC, Cullen SP, Martin SJ. (2008) Apoptosis: Controlled demolition at the cellular level. *Nat. Rev. Mol. Cell Biol.* 9:231–41.
20. Lee EW, Seo J, Jeong M, Lee S, Song J. (2012) The roles of FADD in extrinsic apoptosis and necroptosis. *BMB Rep.* 45:496–508.
21. Aqeilan RI, Calin GA, Croce CM. (2010) miR-15a and miR-16–1 in cancer: Discovery, function and future perspectives. *Cell Death Differ.* 17:215–20.
22. Cimmino A, *et al.* (2005) miR-15 and miR-16 induce apoptosis by targeting BCL2. *Proc. Natl. Acad. Sci. U. S. A.* 102:13944–9.
23. Xia L, *et al.* (2008) miR-15b and miR-16 modulate multidrug resistance by targeting BCL2 in human gastric cancer cells. *Int. J. Cancer.* 123:372–9.
24. National Research Council (U.S.), Committee for the Update of the Guide for the Care and Use of Laboratory Animals, Institute for Laboratory Animal Research (U.S.), National Academies Press (U.S.). (2011) *Guide for the Care and Use of Laboratory Animals*. 8th edition. Washington (DC): National Academies Press.
25. Liang X, *et al.* (2013) p62 sequestosome 1/light chain 3b complex confers cytoprotection on lung epithelial cells after hyperoxia. *Am. J. Respir. Cell Mol. Biol.* 48:489–96.
26. Ryter SW, *et al.* (2007) Mechanisms of cell death in oxidative stress. *Antioxid. Redox Signal.* 9:49–89.
27. Dumont A, *et al.* (1999) Hydrogen peroxide-induced apoptosis is CD95-independent, requires the release of mitochondria-derived reactive oxygen species and the activation of NF-kappaB. *Oncogene*. 18:747–57.
28. Whittemore ER, Loo DT, Watt JA, Cotman CW. (1995) A detailed analysis of hydrogen peroxide-induced cell death in primary neuronal culture. *Neuroscience.* 67:921–32.
29. Heberlein W, Wodopia R, Bartsch P, Mairbaurl H. (2000) Possible role of ROS as mediators of hypoxia-induced ion transport inhibition of alveolar epithelial cells. *Am. J. Physiol. Lung Cell Mol. Physiol.* 278: L640–48.
30. Kang R, Zeh HJ, Lotze MT, Tang D. (2011) The Beclin 1 network regulates autophagy and apoptosis. *Cell Death Differ.* 18:571–80.
31. Driscoll J, Anaissie EJ, Jagannathan S. (2013) Autophagy is uncoupled from ATG5-dependent apoptosis in cells resistant to proteasome inhibition. *Blood.* 122:4448.
32. Palamarchuk A, *et al.* (2010) 13q14 deletions in CLL involve cooperating tumor suppressors. *Blood.* 115:3916–22.
33. Guo CJ, Pan Q, Li DG, Sun H, Liu BW. (2009) miR-15b and miR-16 are implicated in activation of the rat hepatic stellate cell: An essential role for apoptosis. *J. Hepatol.* 50:766–78.
34. Wang H, Yu B, Deng J, Jin Y, Xie L. (2014) Serum miR-122 correlates with short-term mortality in sepsis patients. *Crit. Care.* 18:704.
35. Sirotkin AV, *et al.* (2014) Involvement of microRNA Mir15a in control of human ovarian granulosa cell proliferation, apoptosis, steroidogenesis, and response to FSH. *Microrna.* 3:29–36.
36. Li W, *et al.* (2015) Paeoniflorin inhibits proliferation and induces apoptosis of human glioma cells via microRNA-16 upregulation and matrix metalloproteinase-9 downregulation. *Mol. Med. Rep.* 12:2735–40.
37. Wu G, *et al.* (2011) Hepatitis B virus X protein downregulates expression of the miR-16 family in malignant hepatocytes in vitro. *Br. J. Cancer.* 105:146–53.
38. Cai CK, *et al.* (2012) miR-15a and miR-16-1 downregulate CCND1 and induce apoptosis and cell cycle arrest in osteosarcoma. *Oncol. Rep.* 28:1764–70.
39. Hao R, Hu X, Wu C, Li N. (2014) Hypoxia-induced miR-15a promotes mesenchymal ablation and adaptation to hypoxia during lung development in chicken. *PLoS One.* 9: e98868.
40. Liu L, *et al.* (2014) MicroRNA-15b enhances hypoxia/reoxygenation-induced apoptosis of cardiomyocytes via a mitochondrial apoptotic pathway. *Apoptosis.* 19:19–29.
41. Luo Q, *et al.* (2013) MiR-15a is underexpressed and inhibits the cell cycle by targeting CCNE1 in breast cancer. *Int. J. Oncol.* 43:1212–18.
42. Komabayashi Y, *et al.* (2014) Downregulation of miR-15a due to LMP1 promotes cell proliferation and predicts poor prognosis in nasal NK/T-cell lymphoma. *Am. J. Hematol.* 89:25–33.

Cite this article as: Cao Y, *et al.* (2016) MicroRNA-15a/16 regulates apoptosis of lung epithelial cells after oxidative stress. *Mol. Med*. 22:233–43.